

# Intermediate bands versus levels in non-radiative recombination

Antonio Luque, Antonio Martí, Elisa Antolín\*, César Tablero

*Instituto de Energía Solar, ETSIT, Universidad Politécnica de Madrid, 28040 Madrid, Spain*

Received 16 January 2006; accepted 8 March 2006

## Abstract

There is a practical interest in developing semiconductors with levels situated within their band gap while preventing the non-radiative recombination that these levels promote. In this paper, the physical causes of this non-radiative recombination are analyzed and the increase in the density of the impurities responsible for the mid-gap levels to the point of forming bands is suggested as the means of suppressing the recombination. Simple models supporting this recommendation and helping in its quantification are presented.

© 2006 Elsevier B.V. All rights reserved.

*PACS:* 73.20.jc; 73.20.Fz; 71.55.-i; 73.50.Gr

*Keywords:* Bulk semiconductor; Non-radiative recombination; Intermediate band; Impurity levels; Deep centers; Mott transition

## 1. Introduction

The use of intermediate bands (IB) or levels lying within the band gap of a semiconductor has been proposed [1–3] as a means of manufacturing solar cells with efficiencies of up to 63.3% in ideal conditions. These cells have been implemented with quantum dots that provide the mid-gap level [4], but actual efficiencies have been limited to 10% as a result of weak sub-band absorption and excessive non-radiative recombination among other reasons. We believe that the use of alloys containing a large density of centers able to absorb sub-band gap photons has a higher potential than solutions based on nanotechnology.

Mid-gap levels in semiconductors have been well known for long time. They constitute the so-called deep energy traps and are known to act as very effective recombination centers, thus jeopardizing the potential of IB solar cells.

In this paper we give arguments that suggest that, surprisingly, sufficiently high densities of traps introducing deep energy levels will suppress the non-radiative recombination and thus produce promising IB materials for solar cells.

We looked at this conjecture [5] before publishing the arguments here and have subsequently promoted research, using band calculation methods, for alloys producing a suitable IB [6–11].

Recombination can be radiative and non-radiative. The first mechanism is unavoidable because it is a detailed balance counterpart of the generation through light absorption. A solar cell in which recombination processes are exclusively radiative may reach its efficiency limit [12].

For non-radiative recombination, several mechanisms are known to exist [13–16]. In Auger recombination, the energy of a recombining electron–hole pair is transmitted to another electron. It can be enhanced by impurities but, in general, it is not important except in highly doped semiconductors or at very high levels of carrier injection. In the rest of the non-radiative recombination processes, the energy is transferred to phonons. The statistics of this mechanism were studied in the pioneering works by Shockley, Read and Hall (SRH) [17,18]. However, the physical nature of the mechanism underlying this recombination has remained obscure for years as the energy to be removed from a recombination event is much larger than the energy of a single phonon; in fact, it amounts to a few hundreds of millielectronvolts. For this type of recombination, several mechanisms have been proposed. Among them, the currently most widely accepted one is the lattice

\*Corresponding author. Tel.: +34915441060 x 4322.

E-mail address: [antolin@ies-def.upm.es](mailto:antolin@ies-def.upm.es) (E. Antolín).

relaxation multiphonon emission (MPE) mechanism, which was first proposed by Lang and Henry [19]. They based their work on the early model suggested by Seitz [20], in connection with the quenching of luminescence and which was further developed by Huan and Rhys [21] to explain the absorption line broadening of F-centers in alkaline halides.

The most important points of our argumentation are related to the so-called Anderson [22] and Mott [23] transitions, which determine whether the eigenfunctions of the Hamiltonian of an array of atoms will be a set of wave functions associated to the different atoms or they will be extended wave functions expanding over all the atoms in the array.

This paper is organized as follows: after this introduction we devote a section to refreshing the fundamentals upon which the mechanisms governing the recombination are based, including the use of the so-called configuration diagrams. Then, the lattice relaxation multi-phonon emission mechanism, which is responsible for the SRH recombination, is described. Finally, the argumentation on how to suppress this mechanism is developed, first according to the Anderson mechanisms based on the lack of homogeneity followed by the Mott mechanisms associated to the basic electron–electron interaction. A rough quantification of these effects is introduced, in the first case, with the help of a simplified model.

## 2. Background

### 2.1. Fundamentals

For the analysis of solids, advantage is taken of the big difference in mass between electrons and nuclei. First, a Schrödinger equation associated to the fast electrons is solved in which the positions of the nuclei are taken as parameters that provide the external potential. Once this is done, the electronic energy obtained is introduced into the total Hamiltonian leading to a purely nuclear equation in which the electronic energy appears thus completing the potential energy of the nuclei.

The difference between the aforementioned treatment and the non-approximated Hamiltonian leads to a non-adiabatic term which may be treated as a perturbation that induces transitions from state to state, where the states are those defined in the adiabatic framework.

For the solution of the fast electronic Schrödinger equation, the multi-electronic eigenvectors are split into a set of one-electron eigenvectors (Slater determinants) and a self-consistent calculation [24] is undertaken using one-electron Hamiltonians in which the influence of the other electrons appears as Coulomb repulsion and exchange terms. Every one-electron wave function is expressed as a linear combination of previously selected base functions. The obtained solutions for the one-electron eigenvectors correspond to a given set of nuclei positions. Now we must move the nuclei positions until a lattice-relaxed minimum

energy is achieved for the total nuclei-plus-electrons system.

In the preceding calculation, not all the one-electron eigenstates (as many as base functions) are filled with electrons, but only some of them, up to the number of total electrons in the crystal. Only the filled states participate in the Coulomb repulsion and the exchange terms. Selecting them in order to get the lowest energy is the choice that leads to the calculation of the fundamental state.

In materials with an “impurity”, the impurity produces a potential that is different from those of the host atoms and provides special base functions which are also different from those of the host atoms (if the base function is made up of localized functions, rather than a set of plane waves). For certain impurities, one or several energy eigenvalues will appear in the middle of the semiconductor gap and their eigenfunctions will have a strong projection on the base functions provided by the impurity.

Deep-level impurities, with eigenvalues in the mid-gap, will produce eigenfunctions which are strongly localized and that may be empty and then filled (or vice versa) during the recombination process. In the case of a metallic IB material (e.g. Ti in GaAs and GaP and Cr in ZnS and ZnTe) some filled one-electron wave functions in the fundamental state are in the IB [6–11].

### 2.2. Configuration diagrams

The electronic energy (of all the electrons) for unrelaxed lattice situations becomes a part of the potential energy of the nuclei necessary to study the lattice dynamics. The nuclear energy is usually combined with the electronic energy to draw the so-called “combined potential energy” configuration diagrams. The deviation of the nuclei with respect to their equilibrium position can be expanded to the second order leading to a quadratic form of the combined potential energy of the type  $U = \sum_{i,j} b_{ij} \delta R_i \delta R_j$ . This expression can be represented as a two-dimensional plot if, for example, we set a value for all the  $\delta R_i$  save one. However, the most illustrative of these two-dimensional plots are those representing the potential energy along a line of maximum slope parameterized by  $q$  (the length of the line in the multidimensional  $\delta R_i$  space).

In the configuration diagrams the electronic energy usually refers to a single electron while the nuclear energy is associated to the whole crystal. We can divide the latter by the number of electrons to account for homogeneous concepts.

An example of a configuration diagram is represented in Fig. 1. Let us consider, for the moment, the branches in the figure associated to the valence band (VB) and the conduction band (CB). For them, in the position of equilibrium ( $q = 0$ ), the energy corresponds to the top of the VB and the bottom of the CB. For other values of  $q$ , the branches represent the total potential energy (of electrons and nuclei referred to one electron) as described above and, by definition, the curve in the CB is just a

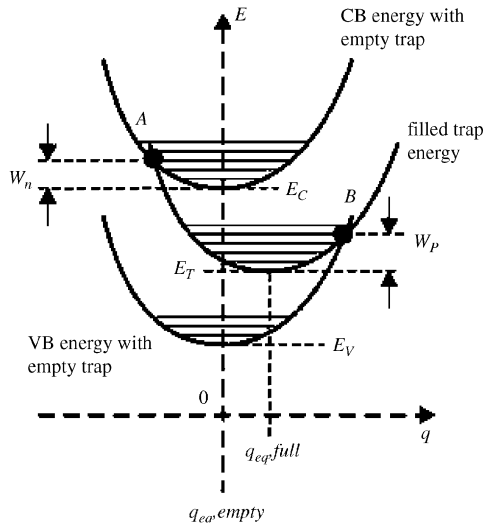


Fig. 1. Configuration diagram illustrating the potential energy of the nuclear equation (including electrons and nuclei) per electron along the line of maximum potential slope parameterized by  $q$ .

vertical displacement of the curve for the VB. The horizontal lines correspond to the total energy determined by the nuclei kinetic energy plus the potential energy.

Let us consider now one impurity with at least one deep-level state which is empty. Let us assume that we fill this virtual deep-level state with one electron. We call this electron a *trapped* electron. The new band calculation will now involve an impurity excited state. Now the Coulomb repulsion and exchange terms have a localized component which is different from those in the fundamental state. As it is widely accepted (which we shall discuss further later in this section), the relaxed position of the impurity atom once it is charged is different from the previous one. For the rest, some changes may also occur, particularly for the neighboring ones but, obviously, most of the atoms in the lattice remain unchanged.

Let us also draw in Fig. 1 the configuration diagram along the line of maximum slope joining the old equilibrium position  $q_{\text{eq,empty}} = 0$  and the new one  $q_{\text{eq,full}} \neq 0$  for the filled trap. This includes the electronic energy of the filled trap at the new relaxation position  $q_{\text{eq,full}}$  plus the total potential energy (per electron)  $U$ . Indeed the  $U$ -shaped curve may have changed with respect to those for the empty trap used for the VB and the CB. However, beyond the displacement we have just described, this change must be small because the number of unmodified electrons is very large. In other words, the  $b$  coefficients can sometimes be considered unchanged.

It is also useful to plot in Fig. 1 the VB and CB combined potential energies (per electron) corresponding to the situation where the trap is empty, as a function of the impurity displacement (along the maximum slope line), and the same function for the trap when it is filled.

This is because, in the subsequent analysis, transitions will occur from band states calculated when the trap is

empty to states in the trap once it is filled and from filled trap states to states in the bands once the trap is emptied.

Huang and Rhys [21], in their pioneering work, evaluated the displacement of the configuration diagram arising from an impurity by considering the crystal as a continuous elastic medium which is polarized by the electric field (potential gradient) created by the impurity. The potential energy obtained using this approach is a quadratic form to which a set of linear terms are added and whose coefficients are a function of the electric field. This, again, represents a quadratic form whose center is displaced by an amount that depends on the electric field plus an “independent” term also dependent on it. This looks similar to what we have drawn in Fig. 1.

### 3. The lattice relaxation MPE non-radiative recombination mechanism

For the explanation of the MPE non-radiative recombination mechanism we refer again to Fig. 1. Note that the trap-full deep-level curve crosses the trap-empty CB curve at point A. By means of non-adiabatic perturbation, transitions are induced between the thermally excited states of electrons in the CB (either the electron or the lattice or both can be excited) to the trap-filled deep-level near point A. Capture cross sections have been calculated under different approximations by several authors [25–31]. In general, it is found that the electron capture cross-section of the SRH statistics has a temperature dependence of the type  $\exp(-W_n/kT)$  (see Fig. 1).

Once the electron is captured in the trap it remains there but the energy lost in the electronic state is largely devoted to keeping the impurity in a violent vibrational state—a “breathing” mode—much stronger than the usual thermal oscillations of the lattice atoms. This strong vibrational state would last forever if the lattice were isolated but, in reality, it is subsequently dissipated by interaction with the electrons in the bands that absorb and emit phonons in the usual way (through the non-adiabatic perturbation) for reestablishing the thermal equilibrium so that, in balance, some few tens of phonons (the Huang–Rhys factor) are emitted after the capture process. This gives its name to the MPE recombination process.

The hole capture is the process by which the filled trap releases its electron to an (unoccupied) VB eigenfunction. To do it, the electron in the trap has to be thermally excited, now essentially by impurity vibrations, until it reaches the vicinity of the energy of point B in Fig. 1. Once the transition is produced, the energy lost by the electronic state is mostly used in a new breathing mode (now around  $q_{\text{eq,empty}} = 0$ ) and subsequently dissipated in the aforementioned way. Here, the hole capture cross-section is proportional to  $\exp(-W_p/kT)$ .

The emission processes are the detailed balance counterparts of the aforementioned capture processes. The SRH statistics can be readily applied. In this case, the trap has an energy  $E_T$  which is that of the minimum of the displaced

curve, when the trap is full. The energy of the trap when it is empty is of little interest in this discussion.

If we summarize the conditions for the MPE mechanism to appear, we must attribute the highest weight to the fact that certain deep-level impurities have a state that is usually empty but can become filled. When this occurs, the new situation of the charge distribution in the crystal is such that the impurity is displaced from its equilibrium position. In a configuration diagram this is revealed by the appearance of the branch of combined potential energy (per electron) of the impurity that presents its minimum out of the fundamental-state equilibrium position. The relaxation to the new position emits enough phonons to justify the electronic energy decrease associated to trapping. In the same way, the return to the equilibrium position when the electron is released to the VB, emits enough phonons to justify the reduction in energy when the electron occupies its final fundamental state position in the VB.

#### 4. Suppressing the lattice relaxation MPE mechanisms

##### 4.1. Disorder-related argumentation

When several atoms are located together, the eigenfunctions belonging to each individual atom become delocalized and are shared by all atoms (as eigenfunctions of the array). In principle this occurs no matter the distance between the atoms of the crystal or cluster of atoms. In practice, leaving aside for the moment the electron–electron interaction, as the atoms may be not exactly equal, the sharing of the eigenfunctions only occurs when the interaction effect is bigger than the natural variations of the individual atoms [22].

This can be applied to the ordinary atoms forming a crystal. As the atoms are close enough to present a strong interaction, the minor variations of the potential resulting from stresses and other imperfections are not able to prevent the individual eigenfunctions to be shared between many atoms and the Bloch-function scheme describes the reality properly.

On the contrary, the impurities, even if they are of the same species, are usually so sparse that their interaction does not prevail over the variations in the single-impurity Hamiltonian resulting from stresses and other imperfections. Consequently, the impurity eigenfunctions remain localized around every individual impurity. This has a very important consequence in the occurrence of the MPE mechanism. As a matter of fact, it provides the electric charge that displaces the impurity from its position when filled with a trapped electron and therefore induces MPE recombination as explained in preceding sections.

Conversely, if an unusually high density of impurities is added, the interaction between the impurities may provoke the sharing of the eigenfunctions between all the impurities and, if this occurs, the charge is distributed between so many impurities in the filling of the trap that no real

change in charge can be observed in any specific location. Consequently, no impurity displacement is produced and the basic mechanism associated to the relaxation to the new position, which is consubstantial to the MPE non-radiative recombination, cannot be produced.

The preceding argumentation is the core of what we want to present in this paper. In what follows we present a simple model to support this argument and also for some attempt at quantification. Later on, we shall discuss the effects of the impurity electron–electron interaction that will complete the argument.

##### 4.2. Model on the localization and delocalization of impurities

Let us consider an array of impurities located in a crystalline-semiconductor host material. We consider this material as providing an external field for the impurity Hamiltonian. The latter will be the sum of a number of single-impurity Hamiltonians  $H_0^{(n)}$  all embedded in the semiconductor material. We shall consider a basis for the problem to be solved made up of the normalized functions  $|m\rangle$  (one per impurity) that are eigenvectors of the single-impurity Hamiltonians of eigenvalue  $E_0^{(n)}$ . These wavefunctions correspond to the trap state that we have been considering in the preceding sections. As they correspond to different Hamiltonians, they are not strictly orthogonal, but if their overlap integral is small, they are nearly so.

Neglecting (for the moment) the electron–electron interaction, the Schrödinger equation for this array is

$$H|\zeta\rangle = \sum_n H^{(n)} \sum_m c_m |m\rangle = E \sum_m c_m |m\rangle. \quad (1)$$

Multiplying on the left by the basis element  $\langle p|$  we get

$$\sum_{n,m} c_m \langle p|H^{(n)}|m\rangle = E \sum_m c_m \langle p|m\rangle. \quad (2)$$

In these equations, when the index of the Hamiltonian,  $n$ , equals either the bra or the ket label ( $p$  or  $m$ ), the corresponding single-impurity eigenvalue,  $E_0^n$  substitutes the Hamiltonian. Eq. (2) can be expressed in a more compact form as

$$Mc = 0, \quad (3)$$

where  $c$  is a column vector whose  $m$  component is  $c_m$  and  $M$  is a square matrix whose non-diagonal element in row  $i$  and column  $j$  is given by

$$M_i^j = (E_0^{(i)} + E_0^{(j)} - E) \langle i|j\rangle + \sum_{k \neq i \neq j} \langle i|H^{(k)}|j\rangle \quad (4)$$

and whose diagonal elements are given by

$$M_i^i = E_0^{(i)} - E + \sum_{k \neq i} \langle i|H^{(k)}|i\rangle. \quad (5)$$

If the impurities are far apart enough to consider that all the overlap integrals or matrix elements with functions of Hamiltonians involving more than one impurity are zero,

then the matrix becomes

$$M = \begin{pmatrix} -E + E_0^{(1)} & 0 & 0 & \cdots \\ 0 & -E + E_0^{(2)} & 0 & \cdots \\ 0 & 0 & -E + E_0^{(3)} & \cdots \\ \cdots & \cdots & \cdots & \cdots \end{pmatrix} \quad (6)$$

which leads to eigenvalues and eigenvectors given by  $E_0^i$  and  $|i\rangle$ , respectively. This means that the different eigenvectors are localized functions around each one of the impurities (except if several or all the energy levels are degenerated). This behavior is found again when the internal products  $\langle ij \rangle$  and matrix elements  $\langle i|H^{(k)}|j \rangle$  with  $k \neq i \neq j$  are small.

#### 4.3. Example of array with exponentially fading interaction

Let us take a three-dimensional array of impurities, defined by a cubic simple translational lattice (for the impurities, not for the host semiconductor) of side  $L$ . The density of impurities is therefore  $N_T = 1/L^3$ . We arbitrarily assume terms for the overlap integrals of the type

$$\langle ij \rangle = P \exp\left(-\frac{|\mathbf{r}_i - \mathbf{r}_j|}{a}\right), \quad (7)$$

$$\langle i|H^{(k)}|j \rangle = H \exp\left(-\frac{|\mathbf{r}_i - \mathbf{r}_j|}{a} - \frac{|\mathbf{r}_i - \mathbf{r}_k||\mathbf{r}_j - \mathbf{r}_k|}{a(|\mathbf{r}_i - \mathbf{r}_k| + |\mathbf{r}_j - \mathbf{r}_k|)}\right), \quad (8)$$

which fade when the wave functions are far away (they do not overlap) or the Hamiltonian is far from both wave functions. In these formulas,  $\mathbf{r}$  represents the position in the array lattice and is a vector of the type:

$$\mathbf{r}_i = \{m_i, n_i, p_i\}L \quad (9)$$

with  $m$ ,  $n$  and  $p$  integers.

Let us consider the finite lattice made up of all the index nodes  $-1, 0$  and  $1$ , amounting to 27 impurity atoms. Eqs. (7) and (8) are then calculated assuming periodic boundaries; that is,  $\langle ij \rangle$  is actually evaluated as  $\langle 0|j-i \rangle$  and any  $\langle i|H^{(k)}|j \rangle$  as  $\langle 0|H^{(k-i)}|j-i \rangle$  (so that any impurity is surrounded by another 26 impurities). Furthermore, we shall assume that there is a linear spread of the isolated impurity eigenvalue  $E_0^{(n)}$  amounting in total to 0.01 eV. This is taken arbitrarily to simulate the effect of stresses and imperfections in the crystal or the way of incorporating the impurities into it. Its influence will be examined later.

The approximate scope of our treatment allows us to use the following simplification which saves a lot of calculations: as the eigenvalues of the isolated atoms are all almost equal and very close to the eigenvalues of the many-impurities problem, we shall use  $(E_0^{(i)} + E_0^{(j)} - E) = E_0$  in Eq. (4). Furthermore we shall set  $P = 1$ ,  $H = E_0$  and  $E_0 = -1$ . We also set  $a = 2 \times 10^{-8}$  which produces an eigenvalue splitting of about 0.1 eV. This is approximately

the split found by band calculations in  $\text{TiGa}_{31}\text{P}_{32}$  [32] for a Ti concentration of 2%.

With these conditions we can now evaluate several situations according to the density of impurities. Fig. 2a, shows the projection  $c_i^*c_i$  of the 10th eigenvector in the base functions around the 27 impurity atoms of the model for a density of impurities of  $N_T = 10^{14} \text{ cm}^{-3}$ . It can be seen that the eigenvector consists of the base wave function around the 10th impurity alone. All the charge of a trapped electron will be located there making it possible for the recombination induced by lattice relaxation MPE to appear. For the other eigenvectors the same occurs around other impurities. In fact, in this case, the matrix is almost purely diagonal. The results of the calculation for a density of impurities  $N_T = 10^{21} \text{ cm}^{-3}$  is shown in Fig. 2b. In this case, the 10th eigenvector does not have a large proportion of it projected on any specific atom. As a matter of fact, almost 30% of the charge is around the 1st atom but, for the remainder, the proportion is lower. For other eigenvectors the localization is smaller still. Most probably the charge would be even more spread out if we took more than the 27 atoms into our calculation. We can thus conclude that for this large density of impurities the displacement of the impurity at the electron capture would be very small or negligible. Thus, the energy  $W_n$  in Fig. 1 would become very high and the electron capture by the

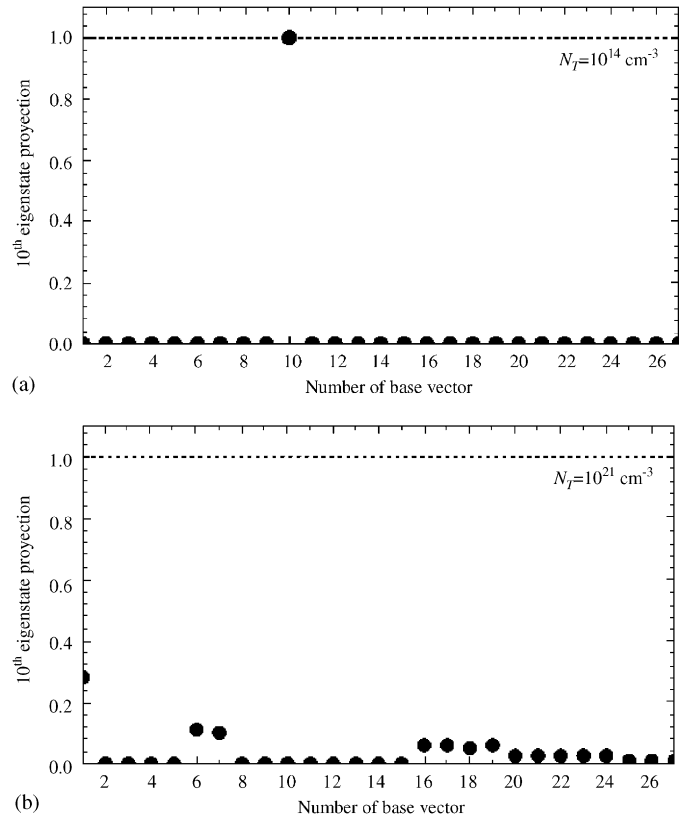


Fig. 2. Projection  $c_i^*c_i$  of the 10th eigenvector in the base functions around the 27 impurity atoms of the model. Data for  $E_0^{(i)} = -1 + 0.01 \times i/27 \text{ eV}$ .  $a = 2 \times 10^{-8} \text{ cm}$ : (a) for a density of traps  $N_T = 10^{14} \text{ cm}^{-3}$ ,  $L/a = 1077.22$  and (b) for a density of traps  $N_T = 10^{21} \text{ cm}^{-3}$ ,  $L/a = 5$ .

impurity would become very unlikely. It is true that the recombination rate in the SRH statistics is proportional to the number of impurities but  $W_n$  would increase to infinity with the decrease in the displacement,  $g_{\text{eq.full}}$ , and the exponential of minus  $W_n$  would decrease even faster so that the capture cross section per impurity will decrease much faster than the increase of impurities.

We have examined how fast this effect occurs based on the model presented here. For densities as high as  $N_T = 10^{20} \text{ cm}^{-3}$ , at least one of the eigenvectors remains localized. The transition seems to occur rather abruptly between  $N_T = 2 \times 10^{20}$  and  $4 \times 10^{20} \text{ cm}^{-3}$ . We have also examined the effect of reducing the spread in energy of the isolated atom eigenvalue to 0.001 eV. (instead of the 0.01 eV used so far). The effect is rather small. The threshold for de-localization is only reduced to the range  $N_T = 1 \times 10^{20} - 2 \times 10^{20} \text{ cm}^{-3}$ .

Until now we have considered a regular array of impurities. We may wonder if this reduction in recombination is associated to this regular nature or just to the proximity of the impurities with no special influence derived from its ordered positions. For this study (with the spread in energy of the isolated atom eigenvalue set to 0.001 eV) we have located the impurities in the aforementioned regular positions but displaced in each coordinate an amount established by a random variable of zero average and equally distributed between  $-0.5$  and  $0.5$  times  $0.1$  (that is, each coordinate is displaced by at most  $\pm 5\%$  of their regular position). The result is that, in this case, the delocalization is more difficult to achieve. In fact, it is not easily achieved at all, no matter the density. It is almost achieved (for most of the eigenvalues but not for all) between  $N_T = 1 \times 10^{20} - 5 \times 10^{20} \text{ cm}^{-3}$ . It seems clear that regularity assists a lot in the delocalization.

It is worth mentioning that the reduction of the non-radiative recombination in a regular structure of impurities should also enhance the radiative recombination [33,34].

#### 4.4. Effect of the electron–electron interaction

The aforementioned arguments neglect the electron–electron interaction. However, even if we assume that the host semiconductor is providing an external field for the impurity wave functions, so that its electrons are not affected by the impurity electrons, these electrons will still interact among themselves. In consequence, many-electron eigenvectors should be considered and treated as described in Section 2.1.

Although this complex treatment is beyond our scope here, it will help us to explain that single–electron eigenfunction localization will be produced when the impurities are sparsely distributed, even if the crystal is perfect and the impurities strictly identical. In this case, the eigenfunctions of all the single–impurity Hamiltonians are all characterised by the same eigenvalue  $E_0^{(n)} = E_0$  that—leaving aside the electron–electron interaction—is also a degenerate eigenvalue of the combined-impurities Hamil-

tonian, whose eigenfunctions are all the kets  $|n\rangle$ . Consequently, any linear combination of these kets is also an eigenfunction and therefore, localized and delocalized eigenfunctions can equally take place. However, when the electron–electron interaction is taken into account, if delocalized functions were accepted as valid solutions, their corresponding eigenvalues would be characterized by higher energies than the localized ones. This is because the overlap between the wave functions that exists in the delocalized case causes a positive contribution to the energy as a result of Coulomb interaction. The localized case is, then, a better solution since it leads to lower energies [35].

However, the eigenfunctions will delocalize when the density of impurities increases. In this we shall follow the original argument by Mott [23]. This argument has been used in numerous cases and, in particular, to determine when donor impurity bands become conductive. To our knowledge it has not been used, even in its more evolved forms [36], to determine when deep center bands become conductive or, what is equivalent, when its electrons become delocalized.

The basis of the argument is as follows: when an electron is removed from an impurity (or atom, in the general argument), the impurity becomes positively charged with an electric charge  $e$  that tends to attract the electron with a potential energy (SI unities)  $-e^2/4\pi\epsilon_0 r$ . This hydrogen-like potential energy presents bound states as well as unbound states, according to well-known formulas. However, the presence of a gas of (potentially) mobile electrons screens the potential and renders it  $-e^2 \exp(-\lambda r)/4\pi\epsilon_0 r$  where  $\lambda$  increases with the mobile electron density. If  $\lambda$  is high enough—approximately the inverse of the Bohr radius—the attracting potential ceases to be able to bound electrons. In this case, the electrons become unbound and a transition to delocalized electrons is produced.

Let us apply this general principle to our deep-trap electrons. The presence of the host semiconductor electrons introduces a dielectric constant  $\epsilon$  (potential energy  $-e^2/4\pi\epsilon\epsilon_0 r$ ) which accounts for the effect caused by the impurity electron in the host material electrons (which so far has been considered as an external potential and therefore not affected by the impurity electron). Unlike in a metal, the host semiconductors, with a full VB and an empty CB, and not having any sensible residual conductivity—because the Fermi level is expected to be situated in the IB[3]—produces no screening [37] of the potential energy. However, the impurity electrons  $|n\rangle$  produce a certain screening with

$$\lambda^2 = \frac{e^2}{\epsilon\epsilon_0} \int \left( -\frac{df(E)}{dE} \right) g(E) dE = \frac{e^2}{\epsilon\epsilon_0} \int \frac{f(1-f)}{kT} g(E) dE, \quad (10)$$

where  $f$  is the occupation Fermi–Dirac function and  $g(E)$  is the IB density of states per unity of energy and volume. Since the IB is very narrow and is crossed by the IB Fermi

level, we can write  $f \cong (1 - f) \cong \frac{1}{2}$  and

$$\lambda^2 \cong \frac{e^2}{\varepsilon\varepsilon_0} \int \frac{g(E)}{4kT} dE \cong \frac{e^2 N_T}{2\varepsilon\varepsilon_0 kT}. \quad (11)$$

Note that the density of states resulting from the spin, is twice the number of traps.

At room temperature,  $kT = 0.025$  eV, the condition for not retaining bound electrons in the impurity is approximately achieved when [23]  $\lambda a_H \cong 0.888$ ,  $a_H = 4\pi\varepsilon\varepsilon_0\hbar^2/m_0e^2$  being the Bohr radius (no effective mass is used here because the electrons concerned do not move in a band). The combination of all this leads to a critical  $N_T = N_{T_{\text{crit}}} = (1.577kT\varepsilon\varepsilon_0/e^2a_H^2)$  which in our case results in  $N_{T_{\text{crit}}} = 5.9 \times 10^{19} \text{ cm}^{-3}$ . This is the value above which the electron becomes delocalized due to the electron–electron interaction. This value is smaller than the one based on the disorder characteristics described in the preceding sections, so it should be dominant.

Note that no argument here is associated to the regular placement of the impurity atoms that, in the Mott scheme, is not expected to affect very much the delocalization of the electrons and consequently the suppression of the MPE recombination.

## 5. Conclusions

We have reviewed the physical nature of the SRH recombination mechanism. It is based on the displacement of the impurity atom when it captures an electron arising from the electric charge carried by this electron. The relaxation of this displacement provides the phonons necessary to compensate for the variations in electronic energy.

Consequently, we have proposed a way of suppressing this mechanism consisting of the increase in the density of impurities to such a level that the distribution of the trapped electron charge density among all the impurities prevents the appearance of strong localized charge variations and thus the displacement of the trapping impurities.

In the light of this paper, it is clear that IB materials exist (which has sometimes been considered doubtful), if we consider the many semiconductors that present deep-level impurities in such a way. The real question is now to what extent must we increase their density to suppress the SRH recombination. A very simple model is presented, based on the existence of crystal imperfections that seem to indicate that at concentrations in the range of  $N_T = 10^{21} \text{ cm}^{-3}$ , or even less, the SRH might become suppressed if the impurity atoms are located regularly. In addition a substantial level of sub-band gap optical absorption (as compared to our present QD IB solar cells [38]) could be produced to make efficient IB cells possible. Furthermore, arguments associated to the Mott transition establish that concentrations of  $5.9 \times 10^{19} \text{ cm}^{-3}$  for the example examined would suffice to suppress this recombination, without sensible influence, we think, of the regularity of their position.

The fulfillment of the conditions requested here is qualitatively equivalent to the condition of having enough interaction of the impurity atoms as to form IBs.

The present conclusion might also be of interest not only for IB solar cells but also for many other semiconductor devices.

## Acknowledgments

This work has been supported by the project FULL-SPECTRUM, funded by the European Commission under Contract No. SES6-CT-2003-502620.

## References

- [1] M. Wolf, Proc. I.R.E. 48 (1960) 1246.
- [2] A. Luque, A. Martí, Phys. Rev. Letts. 78 (1997) 5014.
- [3] A. Luque, A. Martí, Prog. Photovoltaic., Res. Appl. 9 (2001) 73.
- [4] A. Luque, A. Martí, C. Stanley, N. López, L. Cuadra, D. Zhou, A. McKee, J. Appl. Phys. 96 (2004) 903.
- [5] A. Luque, A. Martí, L. Cuadra, in: W.G. Madow (Ed.), Proceedings of the 16th European Photovoltaic Solar Energy Conference, James and James, London, 2000, pp. 59–61.
- [6] P. Wahnón, C. Tablero, Phys. Rev. B Condens. Matter 65 (2002) 1.
- [7] C. Tablero, P. Wahnón, Appl. Phys. Lett. (2003) 151.
- [8] J.J. Fernández, C. Tablero, P. Wahnón, Inter. J. Quantum Chem. 91 (2003) 157.
- [9] C. Tablero, A. García, J.J. Fernández, P. Palacios, P. Wahnón, Comput. Mater. Sci. 58 (2003) 27.
- [10] C. Tablero, Solid State Commun 133 (2005) 97.
- [11] C. Tablero, Phys. Rev. B 72 (2005) 035213.
- [12] A. Martí, G.L. Araújo, Solar Energy Mater. Solar Cells 43 (1996) 203.
- [13] N.F. Mott, Solid State Electron 21 (1978) 1275.
- [14] H.G. Grimmeiss, E. Janzén, Chalcogen-related defects in silicon, in: T.S. Moss (Ed.), Handbook of Semiconductors, vol. 3, North-Holland, Amsterdam, 1994 (Chapter 23).
- [15] H.J. Queisser, Solid State Electron 21 (1978) 1495.
- [16] K.W. Böer, Survey of Physics, Van Nostrand Reinhold, New York, 1973 (Chapter 43).
- [17] W. Shockley, W.T. Read, Phys. Rev. 87 (5) (1952) 62.
- [18] R.N. Hall, Phys. Rev. 87 (2) (1952) 387.
- [19] D.V. Lang, C.H. Henry, Phys. Rev. Lett. 35 (32) (1975) 1525.
- [20] F. Seitz, Trans. Faraday Soc. 35 (1939) 74.
- [21] K. Huan, A. Rhys, Proc. R. Soc. London A 204 (1078) (1950) 406.
- [22] P.W. Anderson, Phys. Rev. 109 (5) (1958) 1492.
- [23] N.F. Mott, Rev. Mod. Phys. 46 (4) (1968) 677.
- [24] A. Szabo, N.S. Ostlund, Modern Quantum Chemistry: Introduction to Advanced Electronic Structure Theory, Dover Publications, Mineola, 1996 (Chapter 3).
- [25] R. Kubo, Y. Toyozawa, Prog. Theor. Phys. 13 (2) (1955) 160.
- [26] G. Rickayzen, Proc. R. Soc. London A 241 (1227) (1957) 480.
- [27] V.A. Kovarskii, Soviet Phys. Solid State 4 (6) (1962) 1200.
- [28] V.A. Kovarskii, E.P. Sinyavskii, Soviet Phys. Solid State 4 (11) (1963) 2345.
- [29] D.V. Lang, C.H. Henry, Phys. Rev. Lett. 35 (22) (1975) 1525.
- [30] C.H. Henry, V.D. Lang, Phys. Rev. B 15 (2) (1977) 989.
- [31] K.B. Ridley, J. Phys. C: Solid State Phys. 11 (1978) 2323.
- [32] P. Palacios, J.J. Fernández, K. Sánchez, J.C. Conesa, P. Wahnón, Phys. Rev. B 73 (2006) 085206.
- [33] A. Martí, L. Cuadra, N. López, A. Luque, Semiconductors 38 (2004) 985.
- [34] A. Martí, L. Cuadra, A. Luque, Intermediate Band Solar Cells, Series in Optics and Optoelectronics, in: A. Martí, A. Luque (Eds.), Next generation photovoltaics: high efficiency through full spectrum

- utilization, Institute of Physics Publishing, Bristol, 2003, pp. 140–162 (Chapter 7).
- [35] L.D. Landau, E.M. Lifshitz, *Quantum Mechanics*, Butterworth Heinemann, Oxford, 2000 (Chapter 3).
- [36] D. Belitz, T.R. Kirkpatrick, *Rev. Mod. Phys.* 66 (2) (1994) 261.
- [37] J.M. Ziman, *Principles of the Theory of Solids*, second ed, Cambridge University Press, Cambridge, 1972 (Chapter 5).
- [38] A. Martí, N. López, E. Antolín, E. Cánovas, C. Stanley, C. Farmer, L. Cuadra, A. Luque, *Thin Solid Films*, December 2005–January 2006, to be published.